Interpretation of EXAFS spectra for sitting-atop complexes with the help of computational methods

Hsiao, Ya-Wen; Ryde, Ulf

Published in:
Inorganica Chimica Acta

DOI:
10.1016/j.ica.2005.11.036

2006

Document Version:
Peer reviewed version (aka post-print)

Interpretation of EXAFS spectra for sitting-atop complexes with the help of computational methods

Ya-Wen Hsiao and Ulf Ryde

Department of Theoretical Chemistry

Lund University

Chemical Centre

P. O. Box 124

S-221 00 Lund

Sweden

Correspondence to Ulf Ryde

E-mail: Ulf.Ryde@teokem.lu.se; Phone: +46 – 46 2224502; Fax: +46 – 46 2224543

2017-03-19

Abstract

The metallation of tetrapyrroles is believed to proceed via a sitting-atop (SAT) complex, in which some of the pyrrole nitrogen atoms are protonated and the metal ion resides above the ring plane. No crystal structure of such a complex has been presented, but NMR and EXAFS (extended X-ray absorption fine structure) data has been reported for Cu^{2+} in acetonitrile, which has been interpreted as the observation of a SAT complex. However, this interpretation has been challenged and other investigations have shown that there are many possible SAT structures. We have recently developed a method to combine quantum mechanical (QM) calculations and EXAFS fits (EXAFS/QM), which in principle is a standard EXAFS fit that employs all multiple-scattering information in an optimum and self-consistent way and uses the QM calculations to ensure that the obtained structures are chemically reasonable. By this approach, we show that out of 15 putative SAT complexes, structures with the copper ion coordinating to two cis pyrrolenine nitrogen atoms and two or three acetonitrile molecules fit the experimental EXAFS spectrum best. However, an equally good fit can be obtained also by a mixture of the reactant and product complexes.

Keywords: sitting-atop complex, EXAFS, haem, ligand exchange, density functional theory.

Introduction

Biological systems heavily rely on cofactors to support the function of the proteins. One of the most common and versatile groups of cofactors are the tetrapyrroles. They are built from a similar framework, consisting of four pyrrole rings fused to a macrocyclic system by four methine linkages. In the centre of this macrocycle a metal ion is normally bound, giving the coenzyme its specific properties. Well-known biological examples of tetrapyrroles are haem, chlorophyll, vitamin B_{12}, and coenzyme F430 [1]. These cofactors are formed by a complicated biosynthetic pathway, consisting of ~10 steps, the first of which are common to all tetrapyrroles. One important and interesting step in this pathway is the insertion of the metal ion. This step has been extensively studied both in solution [2–7] and in biological systems, where the reaction is catalysed by so-called chelatases [8–13].

The metallation of a porphyrin molecule in solution is believed to consist of the following steps [2–7]: deformation of the porphyrin ring, outer-sphere association of the solvated metal ion and the porphyrin, exchange of a solvent molecule with the first pyrrolenine nitrogen atom (i.e. a porphyrin nitrogen atom without any bound hydrogen), chelate-ring closure with the expulsion of more solvent molecules, first deprotonation of a pyrrole nitrogen atom, and second deprotonation of the other nitrogen atom, which will lead to the formation of the metalloporphyrin.

The intermediate formed after the chelate-ring closure is often called the *sitting-atop* (SAT) *complex* [14]. Thus, SAT is a complex of a doubly protonated porphyrin ring with a metal ion, where the latter coordinates to both of the pyrrolenine nitrogen atoms. The protons on the two pyrrole nitrogen atoms prohibits the metal ion to go into the centre of the porphyrin plane; instead, it will reside above the ring plane and form bonds to some solvent molecules. This complex has been much discussed. SAT complexes of porphyrins with Pt^{2+}, Cu^{2+}, and Rh^{+} have been reported [15–17] and kinetic evidence indicates that it exists for some other ions [18–21]. On the other hand, no crystal structure of a SAT complex has been presented.

However recently, SAT complexes of Cu^{2+} with various porphyrins in acetonitrile have been characterised by kinetic measurements, extended X-ray absorption fine structure (EXAFS) spectroscopy, and nuclear magnetic resonance (NMR) [3,22,23]. The authors interpreted the data as a six-coordinate complex with three kinds of Cu–N interactions, viz. bonds to the pyrrolenine nitrogen atoms of the porphyrin (205 pm), equatorial acetonitrile nitrogen atoms (198 pm), and axial acetonitrile nitrogens (232 pm) [3]. These results have recently been challenged, however, suggesting that other species have been observed, e.g. a doubly protonated porphyrin molecule, as well as the reactant and product of the reaction (copper–acetonitrile complexes and the copper porphyrin) [24–26].

Recently, we performed a quantum mechanical (QM) study of SAT complexes of Mg^{2+}, Fe^{2+} and Cu^{2+} with porphine in water and acetonitrile solution [27]. It suggested that there are a large number of possible structures for the SAT complex, with 1–5 solvent molecules, one or two metal ion, and cis or trans protonation of the porphyrin ring. A structure with only one bond between the porphyrin and copper and 3–5 acetonitrile molecules or a structure with two bonds between the cis-protonated porphyrin and copper and 2–4 acetonitrile molecules fitted the experimental EXAFS and NMR data best and were also low in energy. However, it could not be excluded that only the reactants and products were observed. The QM structures were later used to propose a full reaction mechanism for the metallation of porphyrin in water solution [28].

In this paper, we will try to decide which of the theoretical structures [27] fit the experimentally observed EXAFS for Cu^{2+} in acetonitrile [3,22,23]. To this end, we employ a newly developed technique to combine EXAFS refinements with QM calculations [29]. In essence, the QM calculations are allowed to supplement the EXAFS data in the same way as molecular mechanics calculations are used to supplement the experimental data in crystallographic and NMR refinements of protein structures [30,31].

Methods

The EXAFS/QM method

We have recently developed a technique to combine quantum mechanical (QM) geometry optimisations with EXAFS refinement, EXAFS/QM [29]. This method is implemented in the program ComQum-EXAFS. The approach is analogous to the use of molecular mechanics (or even QM [32,33]) to supplement the experimental data in crystallographic and NMR structure refinement [30,31]. For all three methods, there is not enough information in the experimental data to determine the positions of all atoms in the structure (except in the most accurate crystal and NMR structures) [34]. Therefore, computational chemistry is used to make the bond lengths and angles chemically reasonable. Thereby, a structure is obtained that is consistent with both the experiment and computational data.

This is accomplished by defining an energy function

$$E_{\text{tot}} = w_{\text{EXAFS}}\, E_{\text{EXAFS}} + w_{\text{QM}}\, E_{\text{QM}} \qquad (1)$$

Here, E_{QM} is the standard QM energy and E_{EXAFS} is an EXAFS pseudo-energy describing how well the current model (coordinates of all atoms) fit the EXAFS data. There are several such goodness-of-fit parameters, and we have quite arbitrarily selected χ^2, as defined by the IFEFFIT software [35]. These two energies have different units (E_{QM} is in energy units, e.g. kJ/mole, whereas E_{EXAFS} is unit-less. Therefore, the two terms need to be weighted by w_{EXAFS} and w_{QM}, which determines the relative importance of the EXAFS and QM data (strictly speaking, only one weight is needed, but for practical reasons, it is convenient to have two weights [29]). Considering the typical accuracy of the two methods (±2 pm for metal–ligand bond lengths in EXAFS and ±6 pm for the QM optimised structures [34,36–38]), the weights are selected to give metal–ligand distances that are converged towards the EXAFS preference to within 1 pm (this is obtained by increasing w_{EXAFS} until the distances do not change) [29].

The energy function in Eqn. (1) is then used in a standard QM geometry optimisation, in which the forces are calculated by differentiation of this equation. EXAFS forces are obtained by numerical differentiation (with a step length 10^{-4} pm [29]) for the first-shell atoms along the metal-ligand bonds (this gives essentially the same result as a full numerical differentiation in all three Cartesian coordinates but it takes only a third of the time [29]). The

method has been thoroughly tested and has been shown to perform well and give accurate structures for a symmetric Ni(II)N_6 structure and a less symmetric Cu(II)S_2N_2 model complex with known structures [29]. In fact, the EXAFS/QM structure is normally improved over a standard EXAFS structure, because it takes into account all available multiple-scattering information in an optimum way. This is of great significance in the present case, where multiple-scattering paths can be expected to be very important for both the porphyrin and the acetonitrile ligands (both contain second- and third-shell atoms in a nearly linear geometry).

For each model in the present investigation, typically 12 separate EXAFS/QM calculations were performed, using different values of the two weight factors in Eqn. (1): $w_{QM} = 1$, 0.1, and 0.01, and $w_{EXAFS} = 10^{-5}$, 10^{-4}, 10^{-3}, and 10^{-2} (test calculations with $w_{QM} = 0$ were also performed to see how low values of χ^2_{red} can be expected). Only the result with the lowest value of χ^2_{red} is presented (but still with a reasonable ΔE_{QM}, i.e. the QM energy difference between the EXAFS/QM structure and the structure optimised in vacuum).

Model systems

The calculations in this paper are based on the best structures obtained by our previous QM optimisations in vacuum [27]. They are all complexes of Cu^{2+}, acetonitrile (AN, CH_3CN) and porphine ($PorH_2$, i.e. a porphyrin without any side chains; the side-chains are always >600 pm from the metal ion and should therefore not influence the EXAFS spectrum), with two pyrrole rings protonated either in trans or cis. Only solvent molecules in the first coordination sphere were included in the calculations.

Based on our previous results [27], we have restricted the investigation to nine best complexes, which are shown in Figure 1 and described in Table 1: Complexes with the pyrrole rings protonated in trans and with 2–4 AN molecules, complexes with the pyrrole rings protonated in cis and with 2–4 AN molecules (both the cis and trans complexes have two bonds between the porphyrin and copper), and complexes with only one bond between copper and the porphyrin and 3–5 AN molecules (to still give a total coordination number 4–6; in these complexes, the porphyrin ring is protonated in trans). These complexes will be called trans-2, trans-3, trans-4, cis-2, cis-3 cis-4, 1N-3, 1N-4, and 1N-5 in the following

(Figure 1). The 1N complexes are not SAT complexes in the strict sense defined in the introduction, but they still provide a possible interpretation of the experimental data and they are most likely intermediates in the metallation reaction [28].

It should be noted that all complexes with many AN ligands (trans-3, trans-4, cis-4, 1N-4, and 1N-5) were obtained by constrained optimisations in which the five or six Cu–N distances were constrained to values suggested by the EXAFS results [3] ($Cu–N_{Pyrn}$ = 205 pm, equatorial $Cu–N_{AN}$ = 198 pm, and axial $Cu–N_{AN}$ = 232 pm; N_{Pyrn} is the deprotonated pyrrolenine nitrogen atoms in the porphyrin ring; Cu^{2+} is Jahn–Teller unstable – therefore it will typically have four strong equatorial ligands in a square plane and one or two weaker axial ligand orthogonal to this plane; cf. Table 1); otherwise some of the ligands would dissociate. As discussed before [27], this preference of the copper models for a low coordination number may be an artefact of the omission of AN molecules in the outer coordination shells.

In addition, we have also studied possible reactant and product complexes: $Cu(AN)_4^{2+}$, $Cu(AN)_5^{2+}$ (in both square pyramidal and trigonal bipyramidal geometry), $Cu(AN)_6^{2+}$, CuPor, and $CuPorAN_2$. These are also described in Figure 1 and Table 1. The doubly protonated porphyrin molecule, also suggested to have been observed experimentally (by NMR) [24–26] does not involve any Cu ion and is therefore not observed in the EXAFS experiments.

QM calculations

The QM calculations (both vacuum geometry optimisations and in the EXAFS/QM method) were performed with the density functional BP86 method, which consists of Becke's 1988 gradient corrected exchange functional combined with Perdew's 1986 correlation functional [39,40]. These calculations employed the 6-31G* basis set for all atoms, except for Cu, for which we used the DZP basis set [41]. The latter basis set is slightly smaller than the one used in the previous QM investigation [27], because frequency calculations were needed, which are not possible with *f*-type functions. However, the structures reoptimised with this basis set were essentially identical to those obtained with the larger basis set (to within 2 pm in the Cu–N distances) and the energy changed by less than 1 kJ/mole.

BP86 calculations were sped up (by a factor of ~5) by expansion of the Coulomb interactions in auxiliary basis sets, the resolution-of-identity approximation [42,43]. Calibrations have shown that the geometry of the complexes do not change significantly if the basis set is increased [27]. The changes in the geometry was also minimal if the optimisations were performed in a continuum solvent with the same dielectric constant as AN [27]. Therefore, all QM calculations were performed in vacuum.

All the QM calculations were carried out with the Turbomole software, version 5.6 [44]. Unrestricted open-shell theory was employed for all calculations (Cu^{2+} is a doublet). We made use of default convergence criteria, which imply self-consistency down to 10^{-6} Hartree (0.0026 kJ/mole) for the energy and 10^{-3} a.u. (5.0 kJ/mole/Å) for the maximum norm of the gradient.

EXAFS calculations

We used the program FEFF8.20 [45] to calculate the theoretical EXAFS scattering amplitudes and phase shifts. All EXAFS fits were performed with IFEFFIT-1.2.5 software [35]. If not otherwise stated, the EXAFS fits were performed in the following way: Only copper, nitrogen, and carbon atoms were considered (i.e. no hydrogen atoms). All possible paths with up to six scattering legs (NLEG = 6) and with a maximum effective half-path length (RPATH) of 800 pm were generated by FEFF. Paths with χ and curved-wave

amplitudes less than 2.5 and 1% of that of the path with the largest amplitude were discarded (CRITERIA). In practice, IFEFFIT cannot handle more than 256 paths [35]; therefore only the 256 paths with the highest amplitude were included in the fits (with 1–6 % of the maximum amplitude). In the EXAFS/QM calculations, degeneracy, if any, was removed by duplicating the paths.

The present complicated structures, often without any symmetry, provide a challenge for the EXAFS fits, with 4–6 atoms in the first shell, but 20 heavy atoms in the outer shells of the porphyrin ring (at a distance of typically 300–500 pm) and 4–8 additional heavy atoms in the AN ligands (in a linear fashion). Therefore, the SAT models (cis, trans, and 1N structures) have 8–15 shells of single-scattering paths and a multitude of multiple-scattering paths with significant amplitude. Of course, the EXAFS data do not allow the fit of that many parameters (the estimated number of independent degrees of freedom is 29). Therefore, we needed to strongly restrict the number of fitted parameters.

In particular, the Debye–Waller factors (DWFs) of the paths provide a problem, being different for all the individual paths. We solved this problem by employing the QM method also to calculate the DWFs [29]. The FEFF program offers three different methods to obtain DWFs [45], but the standard correlated Debye model does not work properly for non-homogeneous systems. Instead, we used the equation-of-motion method, which has been shown to work properly for a diverse set of model complexes [46]. However, this method requires a set of force constants for all the chemical bonds (and optionally also for the angles) in the molecule. Such force constants are quite hard to obtain by experimental methods, but they can easily be obtained by QM calculations. Therefore, we performed a QM frequency calculation for the vacuum optimised structure of each of the 15 complexes in Figure 1 and extracted force constants for all bonds and angles in the complex, using the method of Seminario [47,48]. These force constants were provided to the FEFF program, leading to a reasonably accurate estimate of the DWFs for all the paths in the complexes [29]. The DWFs were calculated for the experimental temperature (298 K) [3], with the the WMAX and DOSFIT parameters set to 2 and 0.5, respectively. Sample input files for FEFF and IFEFFIT programs are included as supplementary material for the cis-2 complex and they show the

typical size of the calculated DWFs. Our previous calibrations have shown that DWFs estimated by this equation-of-motion method differ from the corresponding fitted factors for first-shell interactions by 10–30% [29]. This may have quite a large influence on the goodness-of-fit parameters (e.g. χ^2_{red}), but it has a negligible effect on the fitted distances (<1 pm).

With these calculated DWFs, only one parameter was fitted by IFEFFIT in the EXAFS/QM approach, viz. a single E_0 for all paths. This makes the fit for all the various complexes identical and therefore the results should be completely comparable. In the pure EXAFS fit, 1–3 shells of Cu–N distances (Cu–N_{Pyrn}, equatorial Cu–N_{AN}, and axial Cu–N_{AN} distances; the same change in bond distance was applied also to the two carbon atoms in the AN molecule, because AN is completely linear) were also fitted in addition to E_0. All coordination numbers were fixed during the fit. Likewise, the amplitude factor S_0^2 was kept at 0.9. For the mixtures, each molecule had its own value of S_0^2, but their sum was still constrained to 0.9.

All EXAFS fits use the experimental data for the putative SAT complex of Cu and tetraphenylporphyrin in acetonitrile described before [3,22,23]. The fitting range was the same as in the original EXAFS investigation, k = 2–14.5 Å^{-1} and R' = 0.8–4.5 Å [3,22,23]. Essentially the same results are obtained if a different fitting range is used (e.g. k = 2–11.0 Å^{-1}; the ordering of the various complexes do not change at all and the fitted distance hardly change, whereas the absolute values of quality criteria change quite strongly). Fitting in k space, instead of R' space, does not change the results.

Result and Discussion

EXAFS fits based on the QM structures

We started the investigation by simply performing an EXAFS fit to each of the 15 QM optimised structures. In these fits, only E_0 was optimised, because DWFs estimated from the calculations were used throughout. All distances and coordination numbers were kept fixed. In this way, all structures were treated on an equal footing, making the comparison more reliable. The results of these calculations are collected in Table 2. It can be seen that the cis-2 complex

gives the best fit (χ^2_{red} = 2.3), followed by the trans-3, cis-4, cis-3, and 1N-4 complexes (χ^2_{red} = 3.3, 3.4, 3.8, and 4.0 respectively). The reactant and product complexes fit the experimental data poorly.

If we fit also 1–3 distances to the first-shell ligands ($N_{Pyrn,}$ as well as equatorial and axial N_{AN} atoms; the latter two distances were also used for the single-scattering paths for the two carbon atoms in the AN molecules, because AN is linear) a similar result is obtained (Table 3). Of course, χ^2 is reduced for all the complexes, but χ^2_{red} (which also takes into account the increased degrees of freedom) is improved only for a third of the complexes. The same five complexes (cis-2, cis-3, trans-3, cis-4, and 1N-4, in this order) are still the best one (with χ^2_{red} = 2.2, 2.7, 3.5, 3.5, and 4.0), but the cis-3 complex has now advanced to the second position. The change in the distances for the equatorial AN ligands are small (0–2 pm), even if the distances vary from 195 to 203 pm. For the Cu–N_{Pyrn} distance, the changes are larger 1–14 pm and as much as 32 pm for the trans-2. For the axial AN ligands, an improvement in χ^2_{red} was found only for the 1N-4 and 1N-5 structures, with an increase of 27 and 20 pm, respectively. However, it should be noted that neither of the fits are full satisfactorily: As is shown in Figure 2, several peaks remain poorly described, although all multiple-scattering paths with up to six legs were included.

We have also tried to improve the fits further by varying additional single-scattering distances (for all SAT models, nearly all porphyrin and AN atoms contribute with significant single-scattering paths). Interestingly, this did not lead to any true improvement in any of the complexes. For most complexes, χ^2_{red} could be reduced (down to 1.8 for the cis-2 complex), but only for changes in distances that lead to chemically unreasonable structures (with severe disruptions in the porphyrin ring, e.g. C–N or C–C bonds that differ by >20 pm from their ideal bond lengths). Therefore, these fits were not considered realistic and the results are not tabulated. Instead, these results indicate a misfit between the experimental spectrum and the studied structures. This can have two explanations: Either the correct structure is not included in the investigation (i.e. among the structures in Figure 1) or the EXAFS spectrum is not of a

single structure but of a mixture of several different structures. These two possibilities will be tested in the next two sections.

EXAFS/QM results

In order to check if other structures may fit the EXAFS results better, we performed a set of calculations with our new EXAFS/QM program. In this approach, we run a geometry optimisation that employs both the QM and EXAFS information. In principle, the EXAFS data is allowed to improve the structure as much as possible, but the QM calculations ensure that the structures are always chemically reasonable (i.e. that the bond lengths and angles are close to ideal). The calculations also ensure that any change in a certain distance, caused by the EXAFS data, is propagated to all other multiple-scattering paths involving that distance in a self-consistent manner, in variance to a standard EXAFS fit. Calculations were started from all the 15 models in Figure 1 and EXAFS forces were calculated for the metal ion and all the first-shell atoms individually (5–7 atoms).

A strong improvement is observed for most of the complexes, but the best ones are still almost the same: The cis-3 complex has the lowest value of χ^2_{red}, 1.6, but that of the cis-2 complex is almost the same (1.7). The cis-4, trans-3, and 1N-4 complexes have somewhat higher values (2.7–3.0). The reactant and product complexes are still appreciably worse than all the SAT structures.

In general, the changes in the Cu–N_{Pyrn} and equatorial Cu–N_{AN} bond lengths are rather small (0–9 pm), but for the weak axial AN ligands, they are frequently larger (up to 36 pm). In two cases (trans-2 and $CuPorAn_2$), larger changes in the Cu–N_{Pyrn} distances are observed (–18 and +21 pm, respectively). For trans-2, it leads to normal (but unfavourable in this crowded complex) Cu–N_{Pyrn} bond lengths of 205 pm, whereas for $CuPorAn_2$, only one of the four Cu–N_{Pyrn} bonds is affected, leading to an unexpectedly long bond (224 pm). In both cases, this is accompanied by the largest observed ΔE_{QM} strain energies, 16 and 20 kJ/mole (ΔE_{QM} is the energy difference of the complex optimised in vacuum and by EXAFS/QM). Of course, less

strained structures can be obtained with smaller values of w_{EXAFS} in Eqn. (1), but this also leads to higher values of χ^2_{red}, indicating a misfit between the EXAFS data and quantum chemistry (i.e. chemical sense).

It is notable that all the EXAFS/QM calculations were performed without any constraints in the Cu–N distances, in variance to the original QM optimisations for five of the complexes (cis-4, trans-3, trans-4, 1N-4, and 1N-5), in which constraints to the originally suggested EXAFS distances were needed to obtain the desired structures (otherwise, the axial ligands dissociated). Interestingly, stable structures with all Cu–N distances shorter than 300 pm were obtained for all complexes, showing that the EXAFS forces are enough to allow for such structures, even if they cannot be found in the QM potential alone.

In a few cases, the structure reorganises completely. This is expected and represents one of the advantages with the EXAFS/QM method – it allows the structure to change qualitatively if the starting structure is incompatible with the EXAFS data. However, in all cases, the resulting structure is identical to one of the other 14 studied structures. This indicates that the selected set of starting structures is essentially complete and that it is unlikely that we have missed any important structure.

The most notable result is the large variation in the optimised Cu–N distances. Thus, the Cu–N_{Pyrn} distances vary from 197 to 205 pm (200–224 pm for $CuPorAn_2$), the equatorial Cu–N_{AN} distances vary from 194 to 207 pm, and the axial Cu–N_{AN} distances from 223 to 285 pm. These are quite different from the originally suggested distances: 205, 198, and 232 pm, respectively [3]. These where interpreted in terms of the trans-4 model, but it can be seen in Table 4 that even this model gives quite different distances (197–204, 198–205, and 227–265 pm). This clearly shows that the interpretation of the EXAFS data strongly depend on the working model of the structure (i.e. the structure fed into FEFF) and that there are numerous local minima in the EXAFS parameter space. Thus, EXAFS distance can only be trusted if a correct model is used and chemical sense is included, e.g. by computational chemistry.

All the EXAFS/QM structures have been obtained with quite strong weights towards the EXAFS data. A way to check that this weight is not too large, so that the structures are no longer chemically reasonable is to calculate the QM energy of the structures compared to the corresponding structure optimised in vacuum. These energies (ΔE_{QM}) are shown in the last row in Table 4. It can be seen that they are all rather small, 0–11 kJ/mole (besides the two cases mentioned above). In general, for reasonable values of the weight factors, the strain energy should be less than 5–7 kJ/mole [29], and this is the case for all complexes, except cis-4, trans-2, trans-3, and $CuPorAn_2$. For one complex, trans-4, ΔE_{QM} is actually negative. The reason for this is that the reference QM structure involved constraints to the originally suggested EXAFS distances and the final EXAFS/QM structure was actually more stable than such a constrained structure.

Thus, we can conclude that the cis-2 and cis-3 structures are the best candidates for the putative SAT complex. Unfortunately, neither of these structures give any fully satisfactorily fit to the experimental EXAFS data (Figure 3). Therefore, it seems that the experimental spectrum may contain a mixture of several different structures.

EXAFS fits of mixtures

As mentioned above, an alternative explanation of the misfit between the experimental and structural data may be that the experiments are performed on a mixture of several species. In fact, it has been suggested that no SAT structure is actually observed but instead a mixture of the reactant and product complexes (as well as a doubly protonated $PorH_2$ molecule) [24–26].

Therefore, we also performed a weighted fit of $CuAn_4$ (or $CuAn_5$ or $CuAn_6$) and $CuPorAn_2$ (or CuPor). The results are shown in Table 5 and it can be seen that the best fit was obtained for 0.5 $CuAn_4$ + 0.4 $CuPorAn_2$, which gave a χ^2_{red} of 2.5, i.e. close to that of the best SAT model, cis-2, with a comparable method (χ^2_{red} = 2.2; cf. Table 3). We also tried mixtures involving cis-2 and $CuAn_4$ (or $CuAn_5$ or $CuAn_6$) and $CuPorAn_2$ (or CuPor), either alone or

both together, but this did not lead to any strong improvement and the fits were strongly dominated by cis-2 (0.7 or higher).

This led us to do a more detailed comparison of the performance of the cis-2 complex and the $CuAn_4$ + $CuPorAn_2$ mixture (also in Table 5) by fitting also some distances and DWFs. It turned out that the cis-2 complex was not sensitive to the DWFs of the first-shell paths, but the mixture was significantly improved. Moreover, if we also fitted a single DWF for all the other paths, both fits were strongly improved. In fact, both systems ended up with exactly the same value of χ^2_{red}, 1.65. This shows that the goodness of the fits is strongly affected by the DWFs . The calculated DWFs for the cis-2 complex are 0.0055-0.0059 (Cu-AN), 0.0053-0.0065 (Cu-N_{Pyrn}), and 0.0114 (average of the other paths), compared to the fitted values of 0.0029, 0.0039, and 0.0106. For the $CuAn_4$ + $CuPorAn_2$ mixture, the calculated DWFs are 0.0035 (N_{Pyrn}), 0.0026 (axial AN), 0.0045 (equatorial AN), and 0.0086 (average of the other paths), compared to the fitted values 0.0037, 0.0026, 0.0027, and 0.0130.

Unfortunately, this leads us to the conclusion that we can still not unambiguously decide whether a SAT complex is observed for Cu^{2+} in acetonitrile or not. It is clear that if it is observed it is undoubtedly of the cis type with two or three AN ligands. However, a mixture of the substrates and the products is predicted to give a very similar EXAFS spectrum, which fits experimentally spectrum equally well. From the comparison of the fits in Figure 4, it is hard to decide which is the better one. Instead, it is clear that both fits are far from perfect – both fits have the proper number of peaks, but most of them are displaced in both radial distance and intensity. The reason for this is probably that the experimental spectrum is quite noisy, as can be seen in the plot of $k^3\chi(k)$ vs. k. Moreover, the experimental sample may be a more complicated mixture of complexes – Cu^{2+} with its strong Jahn–Teller effect is well-known to have very week axial ligands that may form a gradual transition between coordinated and dissociated complexes.

Conclusions

In this paper, we have combined EXAFS fits and computational chemistry to decide which of the previously identified theoretical SAT structures of Cu^{2+} in acetonitrile [27] fit the experimentally observed EXAFS [3,22,23] best. We have shown that several of these structures give reasonable fits to the experimental EXAFS spectrum without fitting anything except E_0. However, the spectrum is only slightly improved by fitting also the distances to the first-shell atoms. In particular, no improvement is obtained if second-shell atoms are also fitted; instead, such a procedure leads to chemically unreasonable bond lengths within the porphyrin ring, indicating a misfit between the experimental and theoretical data.

We therefore also used our recently developed EXAFS/QM method in which the EXAFS and QM data are used in a balanced and self-consistent manner to obtain a complete structure that is the optimum compromise between the EXAFS and QM data. Thereby, we can employ all multiple-scattering information in the structure, while always ensuring that the structure is chemically reasonable. The procedure allows the structure to change qualitatively if there is a misfit between the EXAFS and QM data. By such an approach, significantly improved structures are obtained and we get a measure (ΔE_{QM}) how strained the structure is (i.e. how much it diverge from chemical sense). All these results consistently points out the cis complexes as the best interpretation of the experimental data. However, the fits are still not fully satisfactorily.

Instead, we have shown that fits of an equal quality can be obtained by simply using a mixture of the QM structures of the reactant ($CuAn_4$) and the product ($CuPorAn_2$). However, the fit is still not fully satisfactorily and if further distances are fitted (within the porphyrin ring), chemically unreasonable distances are obtained.

Therefore, we need to conclude that we still cannot with certainty discard or confirm the experimental observation of SAT complexes of Cu^{2+} and tetraphenylporphyrin in acetonitrile

solution. Clearly, none of the 15 complexes in this investigation satisfactorily fits the experimental data. Of course, we can never exclude the possibility that we have overseen the proper SAT structure. However, we have based the investigation on a very extensive QM study of putative SAT structures, involving 34 converged structures and a great number of additional tested structures [27]. From these, we have selected the 15 best structures (in terms of energies and their fit to the experimental data) for this detailed comparison to the EXAFS data. Moreover, we have employed a method (EXAFS/QM) that allows the structure to change during the optimisation, and we have shown that in the few cases where the structure actually changes, it only gives another structure already considered. This makes it quite unlikely that we have missed any important structure. Instead, a more probable reason for the misfit is that the experimental data represents a mixture of several chemical species, e.g. with a varying number of axial ligands. This, in combination with the problem of estimating reasonable values of the DWFs (especially for the multiple-scattering paths) and the rather poor quality of the EXAFS data, may explain the poor fit of the experimental EXAFS spectrum.

In conclusion, we find no certain evidence for that a SAT complex of any type is observed experimentally for Cu^{2+} in acetonitrile. Instead, the present results indicate that the experimental data is equally well interpretations as a mixture of the reactant and products, as well as the doubly protonated porphyrin, as has been suggested before [22–24]. This is the best conclusion that can be reached by the available EXAFS data and it is based on a method that takes into full account all the available multiple-scattering information in the data.

Finally, we believe that the present application nicely illustrates the strength of the EXAFS/QM method [29]. EXAFS fits traditionally only give quite restricted (but very precise) information about the nearest neighbours of the metal of interest and it is quite hard to take advantage of the detailed information in the spectra (angular information from multiple-scattering paths) without the use of a full atomic model of the sample. Moreover, many nuclear configurations may give fits of a similar quality to the EXAFS data. The

EXAFS/QM method solves several of these problems: It gives a full atomic model of the complexes (coordinates of all atoms). By employing such an atomic model of the complex and explicit numerical EXAFS forces, we get a completely consistent description of the complex that actually is better than that obtained from a standard EXAFS fit, even without any QM information (because changes in the length of one path is automatically propagated to all other paths involving that distance). Moreover, the atomic model allows us to fully employ all information available in the multiple-scattering paths.

In addition, the QM data provides several advantages. First, the QM geometry optimisations provide us with starting structures involving a full atomic detail. It should be noted that the data in Table 2 and 3 entirely rely on starting structures from QM. Second, the QM data ensure that the structures are always chemically sensible even when the distances are allowed to change to improve the fit to EXAFS data. Even better, the QM calculations provides a measure (ΔE_{QM}) of how chemically sensible the structure is. Experience has shown that $\Delta E_0 < 5–7$ kJ/mole for reasonable structures (owing to small, but systematic, errors in the QM method).

Third, the QM method allows us to estimate reasonable DWFs for all paths. This is mandatory in an investigation including multiple-scattering because the number of paths rapidly grows larger than the number of independent degrees of freedom in the experimental data. Moreover, the DWFs of the paths often have quite varying magnitudes making it hard to guess their values.

The only disadvantage with the EXAFS/QM method is that it does not provide structures that are required by the experimental data, only structures that are consistent with the data, i.e. the best possible structure involving the including atoms and reasonably close to the starting structure [29]. However, this is a rather small disadvantage that also applies to normal EXAFS fits. It is solved by testing and comparing several reasonable structures, as in the present investigation. Of course, the EXAFS/QM method is appreciably more time consuming than a standard EXAFS fit. For the present models, the calculations took between one hour and two days, depending on the size of the model and the number of iterations before convergence on a standard personal computer (~2.5 GHz). Calculations with different w_{QM} and w_{EXAFS} weights

can trivially be run in parallel.

In conclusion, we believe that the EXAFS/QM method may become a standard tool in the interpretation of EXAFS spectra. In particular, it is a very powerful method in cases similar to the present, where the goal is to decide which of a number of possible structures fit experimental EXAFS data best.

Acknowledgements

This investigation has been supported by grants from the Swedish research council and by computer resources of Lunarc at Lund University. We thank Prof. Yasuhiro Inada for providing us the EXAFS raw data.

Supplementary material

Sample input files (feff.inp, spring.inp, and ifeffit.inp) for the FEFF and IFEFFIT programs for the cis-2 complex.

References

1. L.R. Milgrom (1997) "The colours of life", Oxford University Press.
2. D.K. Lavallee, Coord. Chem. Rev. 61 (1985) 55-96.
3. M. Inamo, N. Kamiya, Y. Inada, M. Nomura, S. Funahashi Inorg. Chem. 40 (2001) 5636-5644.
4. P. Hambright in K. Smith, (Ed.) Dynamic coordination chemistry of metalloporphyrins, Elsevier, Amsterdam, 1975, pp. 233-278.
5. P. Hambright, J. Am. Chem. Soc. 96 (1974) 3123-3131.
6. D.K. Lavallee in J.F.Liebmann, A. Greenberg, (Eds.) Molecular structure and energetics, vol. 9: Mechanistic Principles of Enzymatic Activity, VCH, New York, 1988, pp. 279-314.
7. S. Funahashi, Inada, Y. Inamo, M. Analyt. Sci. 17 (2001) 917-927.
8. C.J. Walker, Willows RD Biochem J 327: (1997) 321–333
9. H.L. Shubert, Raux E, Wilson KS, Warren MJ Biochemistry 38: (1999) 10660–10669
10. E. Raux, H.L. Schubert, M.J. Warren, Cell Mol Life Sci 57: (2000) 1880–1893
11. C.-K. Wu, H.A. Dailey, J.P. Rose, A. Burden, V.M. Sellers, B.-C. Wang, Nature Str. Biol. 8: (2001) 156–160
12. S. Al-Karadaghi, M. Hansson, S. Nikonov, B. Jonsson, L. Hederstedt, Structure 5 (1997) 1501–1510
13. H.L. Schubert, E. Raux, A.A. Brindley, H.K. Leech, K.S. Wilson, C.P. Hill, M.J. Warren, EMBO J 21 (2002) 2068–2075
14. E.B. Fleischer, J.H. Wang, J. Am. Chem. Soc. 82 (1960) 3498.
15. J.P. Marcqet, T. Theophahanides, Can. J. Chem. 51 (1973) 219.
16. K. Letts, R.A. Mackay, Inorg. Chem. 14 (1975) 2993.
17. E.B. Fleischer, F. Dixon, Bioinorg. Chem. 7 (1977) 129.
18. T.P.G. Sutter, P. Hambright, Inorg. Chem. 31 (1992) 5089-5093.
19. Y. Inada, Y. Sugimoto, Y.Nakano, S. Funahashi, Chem. Lett. (1996) 881-882.
20. J. Takeda, T. Ohya, M. Sato, Inorg. Chem. 31 (1992) 2877-2880.

21. S. Funahashi, Y. Yamaguchi, M. Tanka, Bull. Chem. Soc. Jpn, 57 (1984) 204-208.

22. Y. Inada, Y. Sugimoto, Y. Nakano, Y. Itoh, S. Funahashi, Inorg. Chem. 37 (1998) 5519-5526.

23. Y. Inada, Y. Nakano, M. Inamo, M. Nomura, S. Funahashi Inorg. Chem. 39,(2001) 4793-4801.

24. C.-H. Tsai, J.-Y. Tung, J.-H. Chen, F.-L. Liao, S.-L.Wang, S.-S.Wang, L.-P. Hwang, C.-B. Chen, Polyhedron, 19 (2000) 633-639.

25. H. Baker, P. Hambright, L. Wagner, J. Am. Chem. Soc. 98 (1973) 5942-5946.

26. D.K. Lavallee, M.J. Bain-Ackerman, Bioinorg. Chem. 9 (1978) 311-321.

27. Y. Shen & U. Ryde (2004) J. Inorg. Biochem., 98, 878-895.

28. Y. Shen & U. Ryde (2005) Chem. Eur. J., 11, 1549-1564.

29. Y.-W. Hsiao, Y. Tao, J. E. Shokes, R. A. Scott, and U. Ryde (2005) "EXAFS structure refinement supplemented by computational chemistry", Inorg. Chem., submitted. *A preprint of this paper can be found in http://www.teokem.lu.se/~ulf/cqe.pdf*

30. G. J. Kleywegt, T. A. Jones, "Model building and refinement practice", Meth. Enzym. 1997,227, 208—230

31. J. Cavanagh, W. J. Fairbrother, A. G. Palmer, N. J. Skelton, Protein NMR spectroscopy. Principles and practice, Academic Press, London, 1996

32. U. Ryde, L. Olsen & K. Nilsson (2002) "Quantum chemical geometry optimisations in proteins using crystallographic raw data", J. Comp. Chem., 23, 1058-1070.

33. Y.-W. Hsiao, U. Ryde & T. Drakenberg (2005) J. Biomol. NMR, 31, 97-114.

34. J. E. Penner-Hahn, "X-ray absorption spectroscopy in coordination chemistry", Coord. Chem. Rev., 1999, 190—192, 1101—1123.

35. M. Newville (2001) J. Synchrotron Rad., 8, 322.

36. R. A. Scott, Meth. Enzym. 117 (1985),414—459.

37. E. Sigfridsson, M. H. M. Olsson & U. Ryde (2001) "A comparison of the inner-sphere reorganisation energies of cytochromes, iron-sulphur clusters, and blue copper proteins", J. Phys. Chem. B, 105, 5546-5552.

38. U. Ryde & K. Nilsson (2003) "Quantum chemistry can improve protein crystal structures locally", J. Am. Chem. Soc., 125, 14232-14233.
39. A.D. Becke, Phys. Rev. A, 38 (1988) 3098.
40. J. P. Perdew, Phys. Rev. B, 33 (1986) 8822.
41. A. Schäfer, H. Horn, R. Ahlrichs, J. Chem. Phys. 97 (1992) 2571.
42. K. Eichkorn, Treutler, O.H. Öhm, M. Häser, Ahlrichs, R. Chem. Phys. Lett. 240 (1995) 283-290.
43. K. Eichkorn, F. Weigend, O. Treutler, R. Ahlrichs, Theor. Chem. Acc. 97 (1997) 119.
44. R. Ahlrichs, M. Bär, M. Häser, H. Horn, C. Kölmel, Chem. Phys. Lett. 162 (1989) 165.
45. A. Ankudinov, C. Bouldin, J. J. Rehr, J. Sims, H. Hung (2002) Phys. Rev. B, 65, 104107.
46. A. V. Poiarkonv, (1999) “X-ray absorption spectroscopy fine structure Debye-Waller factors”, Ph.D. Thesis, University of Washington.
47. J. M. Seminario (1996) Intern. J. Quantum Chem., Quantum Chem. Sympos., 30, 59-65.
48. K. Nilsson, D. Lecerof, E. Sigfridsson & U. Ryde (2003) Acta Crystallogr. D, 59, 274-289.

Table 1. Metal–ligand distances (pm) in the optimised SAT structures with Cu^{2+} and AN, optimised by pure QM in vacuum. N_{pyrn} and N_{Pyr} are the pyrrolenine and pyrrole nitrogen atoms in the porphyrin ring (i.e. the nitrogen atoms without or with a hydrogen atom). Distances in bold face without any decimal have been constrained to the suggested EXAFS distances in the optimisation (otherwise these ligands dissociate) [27].

Complex	Metal–ligand distance (pm)		
	N_{Pyrn}	N_{Pyr}	N_{An}
cis-2	201.4, 204.2	317.2, 329.3	199.4, 200.3
cis-3	207.0, 207.4	332.1, 333.6	202.8, 203.2, 225.2
cis-4	**205, 205**	367.0, 368.3	**198, 198, 232, 232**
trans-2	223.4, 223.3	282.2, 282.2	198.9, 198.9
trans-3	**205, 205**	263.5, 302.1	**198, 198, 232**
trans-4	**205, 205**	309.5, 310.0	**198, 198, 232, 232**
1N-3	208.2, 457.9	361.6, 375.3	198.5, 200.2, 200.2
1N-4	**205**, 453.9	364.9, 365.0	**198, 198, 232, 232**
1N-5	**205**, 488.6	391.4, 392.6	**198, 198, 198, 232, 232**
CuPor	202.6*4	–	–
$CuPorAn_2$	203.2*4	–	297.0, 297.4
$CuAn_4$	–	–	196.2, 196.2, 196.2, 196.2
$CuAn_5$ tbp	–	–	197.6, 197.6, 205.5, 205.5, 205.5
$CuAn_5$ sqpy	–	–	199.4, 199.5, 199.6, 199.6, 215.2
$CuAn_6$	–	–	200.6, 200.6, 200.6, 200.6, 238.3, 238.8

Table 2. Results of the EXAFS fits to the QM optimised structures without fitting any distances (i.e. only E_0 was fitted).

Complex	E_0	χ^2	χ^2_{red}	R_{factor}
cis-2	12.8	63	2.26	0.107
cis-3	17.2	105	3.76	0.178
cis-4	12.9	95	3.39	0.161
trans-2	15.5	328	11.74	0.557
trans-3	12.9	92	3.29	0.156
trans-4	13.5	137	4.90	0.232
1N-3	12.6	111	3.97	0.188
1N-4	11.3	201	7.18	0.341
1N-5	11.4	133	4.76	0.226
CuPor	16.6	632	22.64	1.073
$CuPorAn_2$	17.6	822	29.41	1.394
$CuAn_4$	8.7	533	19.08	0.905
$CuAn_5$ tbp	14.4	403	14.42	0.683
$CuAn_5$ sqpy	13.6	377	13.48	0.639
$CuAn_6$	13.5	309	11.05	0.524

Table 3. Results of the EXAFS fits to the QM optimised structures, in which the distances to the first-sphere ligands were fitted (in addition to E_0). Error ranges are given for the fitted distances.

Complex	E_0	χ^2	χ^2_{red}	R_{factor}	Cu – N distance (pm)					
					N1	N2	N3	N4	N5	N6
cis-2	12.6	57	2.19	0.096	197 ± 1	198 ± 1	203 ± 1	206 ± 1		
cis-3	14.6	70	2.71	0.119	202 ± 3	203 ± 3	201 ± 4	201 ± 4	225	
cis-4	12.1	90	3.48	0.153	198 ± 1	198 ± 1	203 ± 2	203 ± 2	232	232
trans-2	10.5	218	8.39	0.369	199 ± 3	199 ± 3	256 ± 6	256 ± 6		
trans-3	12.3	90	3.47	0.153	197 ± 1	197 ± 1	204 ± 1	204 ± 1	232	
trans-4	13.0	135	5.20	0.229	198 ± 2	198 ± 2	204 ± 2	204 ± 2	232	232
1N-3	12.1	105	4.03	0.177	199 ± 5	195 ± 5	196 ± 20	201 ± 20		
1N-4	8.7	131	5.25	0.222	199 ± 4	199 ± 4	198 ± 13	259 ± 6	259 ± 6	
1N-5					198 ± 1	198 ± 1	198 ± 1	207 ± 4	252 ± 8	252 ±
	10.7	124	4.99	0.211						8
CuPor	14.5	624	23.17	1.059	201 ± 1	201 ± 1	201 ± 1	201 ± 1		
$CuPorAn_2$					202 ± 1	202 ± 1	202 ± 1	202 ± 1	287 ± 4	287 ±
	15.2	609	23.49	1.034						4
$CuAn_4$	9.1	530	19.68	0.899	197 ± 1	197 ± 1	197 ± 1	197 ± 1		
$CuAn_5$ tbp	13.3	386	14.89	0.655	197 ± 2	197 ± 2	203 ± 2	203 ± 2	203 ± 2	
$CuAn_5$ sqpy	13.0	359	13.84	0.609	199 ± 1	199 ± 1	200 ± 1	200 ± 1	229 ± 11	
$CuAn_6$					200 ± 1	200 ± 1	200 ± 1	200 ± 1	232 ± 5	232 ±
	13.8	287	11.08	0.488						5

Table 4. Results of the EXAFS/QM calculations.

Complex	E_0	χ^2	χ^2_{red}	R_{factor}	Cu – N distance (pm)						ΔE_{QM}
					N1	N2	N3	N4	N5	N6	kJ/mole
cis-2	11.2	47	1.7	0.079	194.4	200.6	201.8	203.0			1.3
cis-3	12.7	45	1.6	0.076	199.1	200.1	202.6	202.7	233.8		2.8
cis-4	13.0	75	2.7	0.127	199.4	201.6	197.2	205.3	232.9	234.1	11.1
trans-2	15.4	149	5.3	0.252	199.7	199.9	205.3	205.3			15.5
trans-3	11.2	82	3.0	0.140	195.8	197.2	203.4	203.7	231.3		8.1
trans-4	13.8	137	4.9	0.232	196.9	203.9	198.4	205.3	227.3	265.1	–3.6
1N-3	12.2	104	3.7	0.176	200.5	200.8	201.1	201.3			1.3
1N-4	11.6	84	3.0	0.143	200.1	200.1	200.7	250.5	267.7		2.0
1N-5	13.2	107	3.8	0.182	196.1	201.7	202.5	203.2	222.8	243.0	0.9
CuPor	15.2	615	22.0	1.043	201.4	201.4	201.4	201.4			0.5
$CuPorAn_2$	20.8	215	7.7	0.364	199.5	206.1	224.3	205.6	284.8	284.8	20.2
$CuAn_4$	12.2	508	18.2	0.863	199.3	199.3	199.3	199.3			2.1
$CuAn_5$ tbp	13.2	240	8.6	0.407	201.8	202.0	196.6	198.1	228.6		2.7
$CuAn_5$ sqpy	13.9	218	7.8	0.369	202.9	194.6	203.1	200.5	229.6		4.6
$CuAn_6$	15.4	186	6.7	0.316	198.1	207.5	201.9	199.5	229.1	239.1	1.7

Table 5. Results of the EXAFS fits to mixtures. If not otherwise stated, E_0 as well as 2–6 first-sphere Cu–N distances were fitted. The corresponding fits for the cis-2 complex alone are also included for comparison.

Complex			S_0^2			E_0	χ^2	χ^2_{red}	R_{factor}
1	2	3	1	2	3				
$CuAn_6$	CuPor		0.58	0.32		16.0	105	4.39	0.200
$CuAn_6$	$CuPorAn_2$		0.50	0.40		15.8	94	3.93	0.160
$CuAn_5$ tbp	CuPor		0.45	0.45		13.6	145	6.07	0.247
$CuAn_5$ sqpy	CuPor		0.52	0.38		15.5	138	5.75	0.233
$CuAn_4$	CuPor		0.48	0.42		13.0	71	2.86	0.121
$CuAn_4$	$CuPorAn_2$		0.50	0.40		12.5	60	2.52	0.102
$CuAn_4$	$CuPorAn_2$	(a)	0.46	0.44		11.9	49	2.32	0.083
$CuAn_4$	$CuPorAn_2$	(b)	0.45	0.45		12.3	33	1.65	0.056
cis-2	CuPor		0.76	0.14		13.0	46	1.91	0.077
cis-2	$CuPorAn_2$		0.77	0.13		12.6	43	1.87	0.073
cis-2	$CuAn_6$		0.85	0.05		12.5	57	2.36	0.096
cis-2	$CuPorAn_2$	$CuAn_6$	0.69	0.14	0.07	13.0	42	2.11	0.071
cis-2	$CuPorAn_2$	$CuAn_4$	0.70	0.10	0.10	12.3	48	2.11	0.082
cis-2			0.90			12.6	57	2.19	0.096
cis-2	(c)		0.90			12.4	57	2.37	0.096
cis-2	(d)		0.90			11.1	38	1.65	0.064

(a) In this fit, three DWFs were also fitted, viz. for the Cu–N_{AN} path in $CuAn_4$ and for the Cu–N_{Pyrn} and Cu–N_{AN} paths in $CuPorAn_2$.

(b) In this fit, four DWFs were also fitted, viz. the same as in footnote (a) above and a fourth DWF for all the other paths in both complexes.

(c) In this fit, two DWFs were also fitted, viz. for the Cu–N_{Pyrn} and Cu–N_{AN} paths.

(d) In this fit, three DWFs were also fitted, viz. the same as in footnote (c) above and a fourth DWF for all the other paths.

Figure 1. Complexes considered in this investigation.

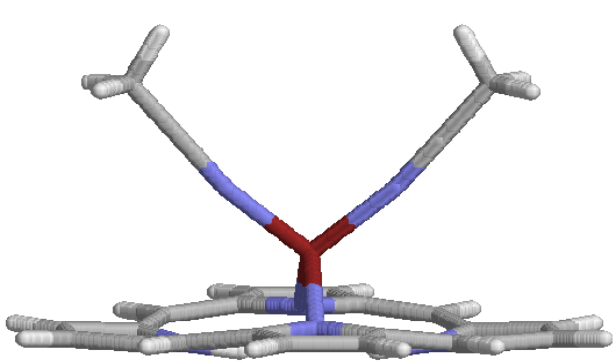

trans-2

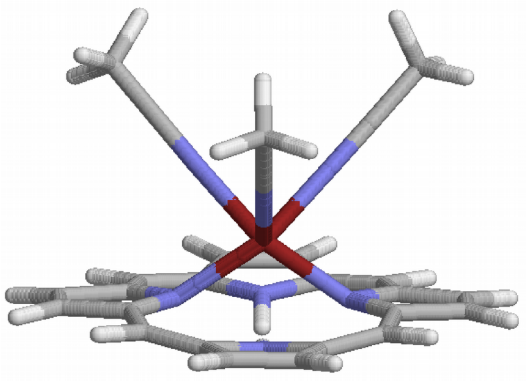

trans-3

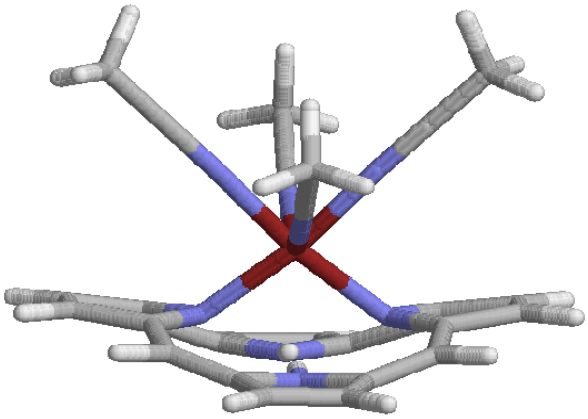

trans-4

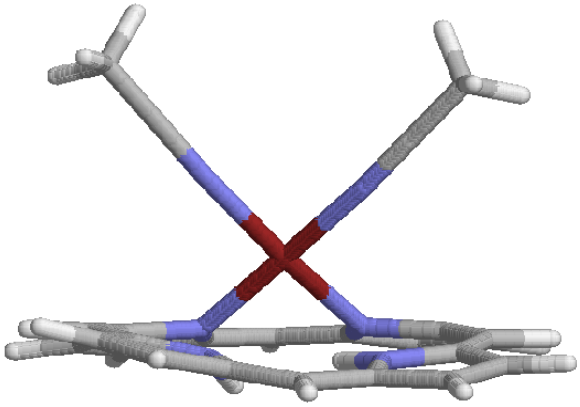

cis-2

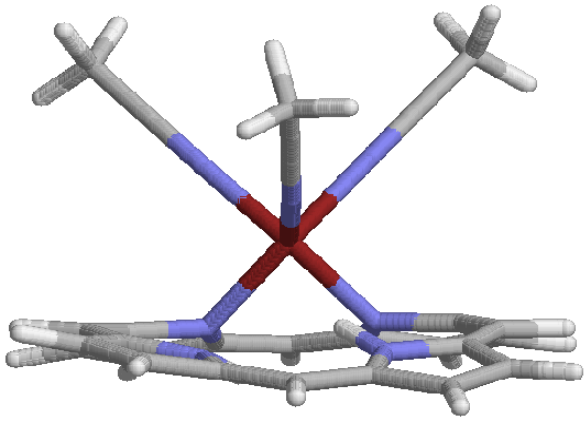

cis-3

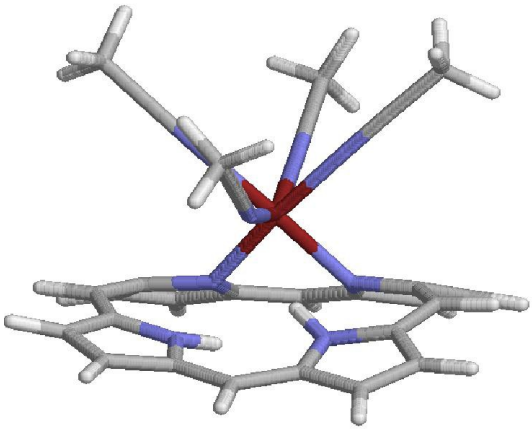

cis-4

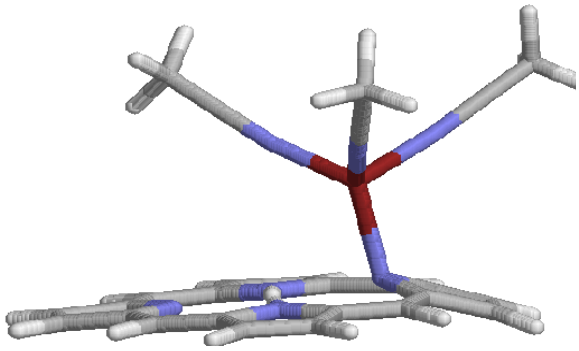

1N-3

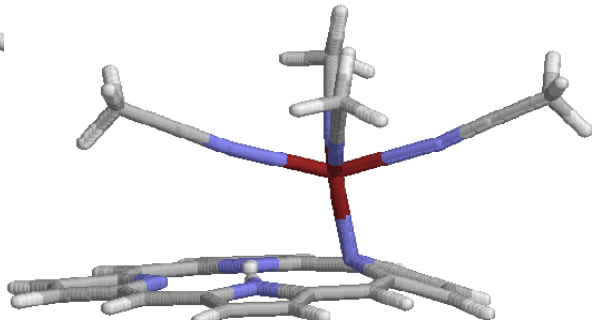

1N-4

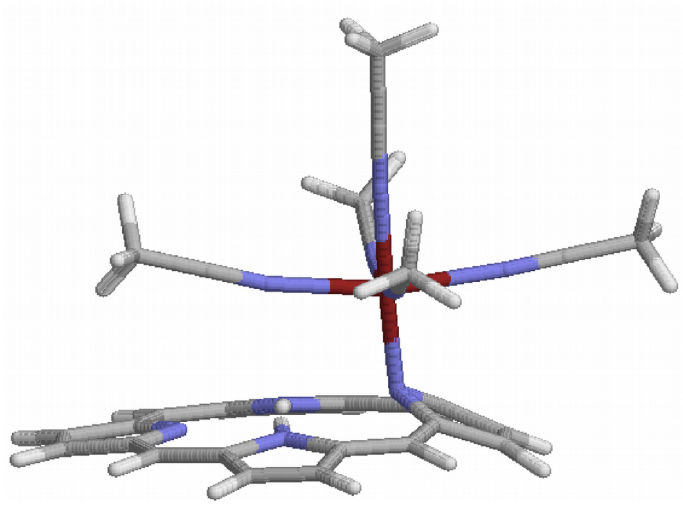

1N-5

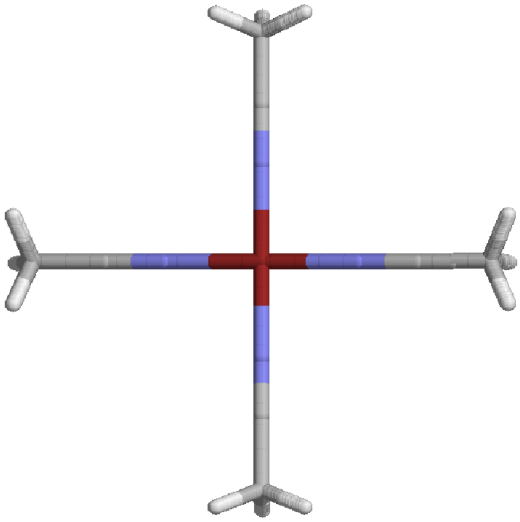

$Cu(AN)_4^{2+}$

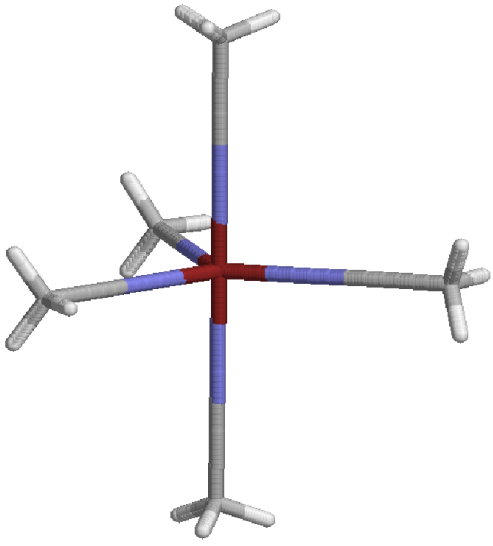

$Cu(AN)_5^{2+}$ trigonal bipyramidal

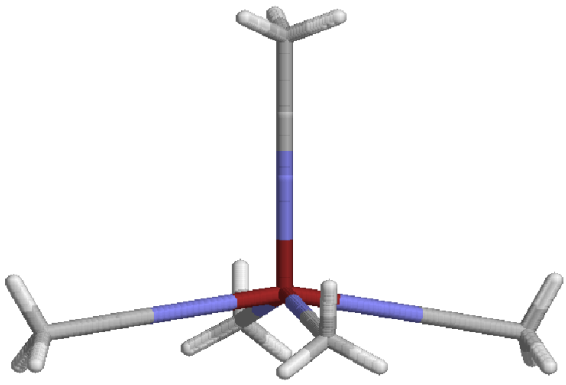

$Cu(AN)_5^{2+}$ square pyramidal

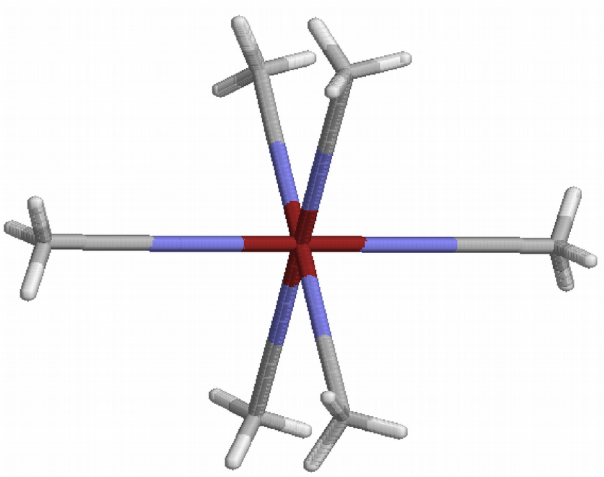

$Cu(AN)_6^{2+}$

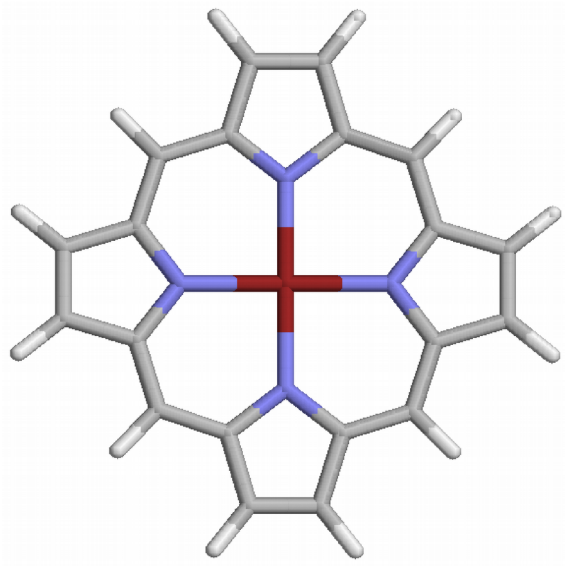

CuPor

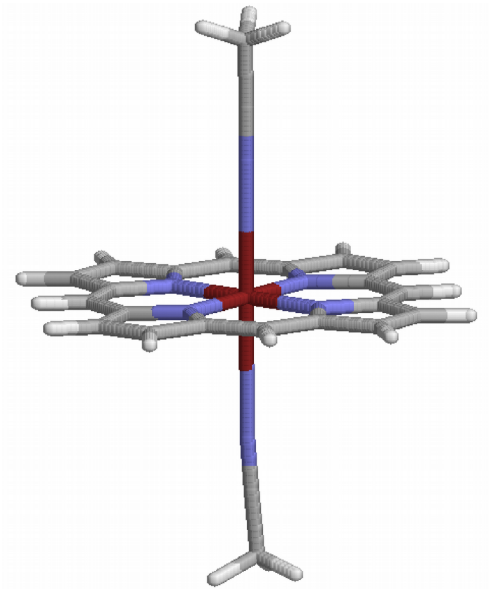

$CuPorAn_2$

Figure 2. Comparison of the EXAFS raw data (blue) and the fit of cis-2 complex, involving E_0 and two Cu–N distances (red), displayed as Fourier-transformed magnitude (k^3-weighted, no phase correction) vs. R', and $k^3\chi(k)$ vs. k.

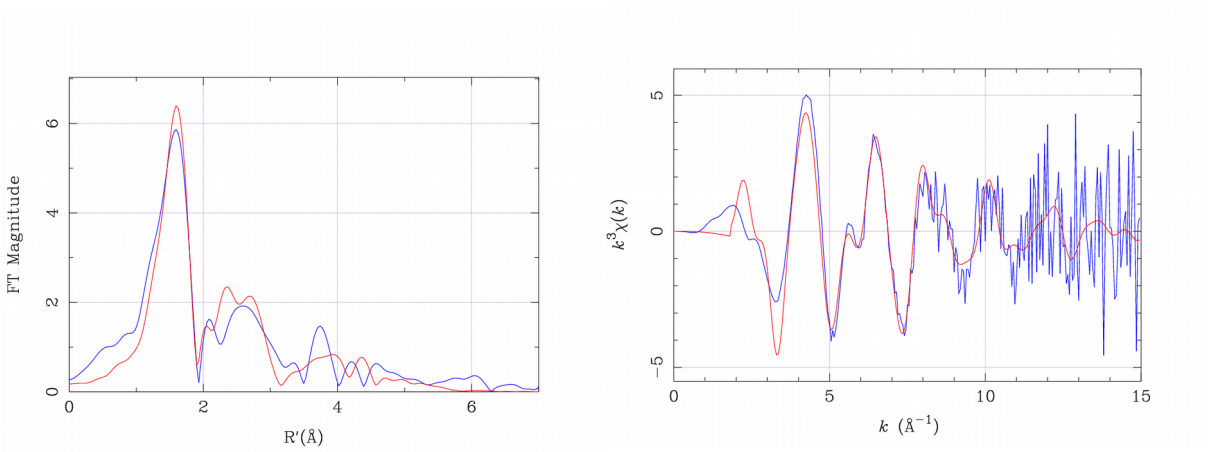

Figure 3. A comparison of the EXAFS raw data (blue) and the EXAFS/QM structure of the cis-2 (a) and cis-3 (b) complexes (red), displayed as Fourier-transformed magnitude (k^3-weighted, no phase correction) vs. R', and $k^3\chi(k)$ vs. k.

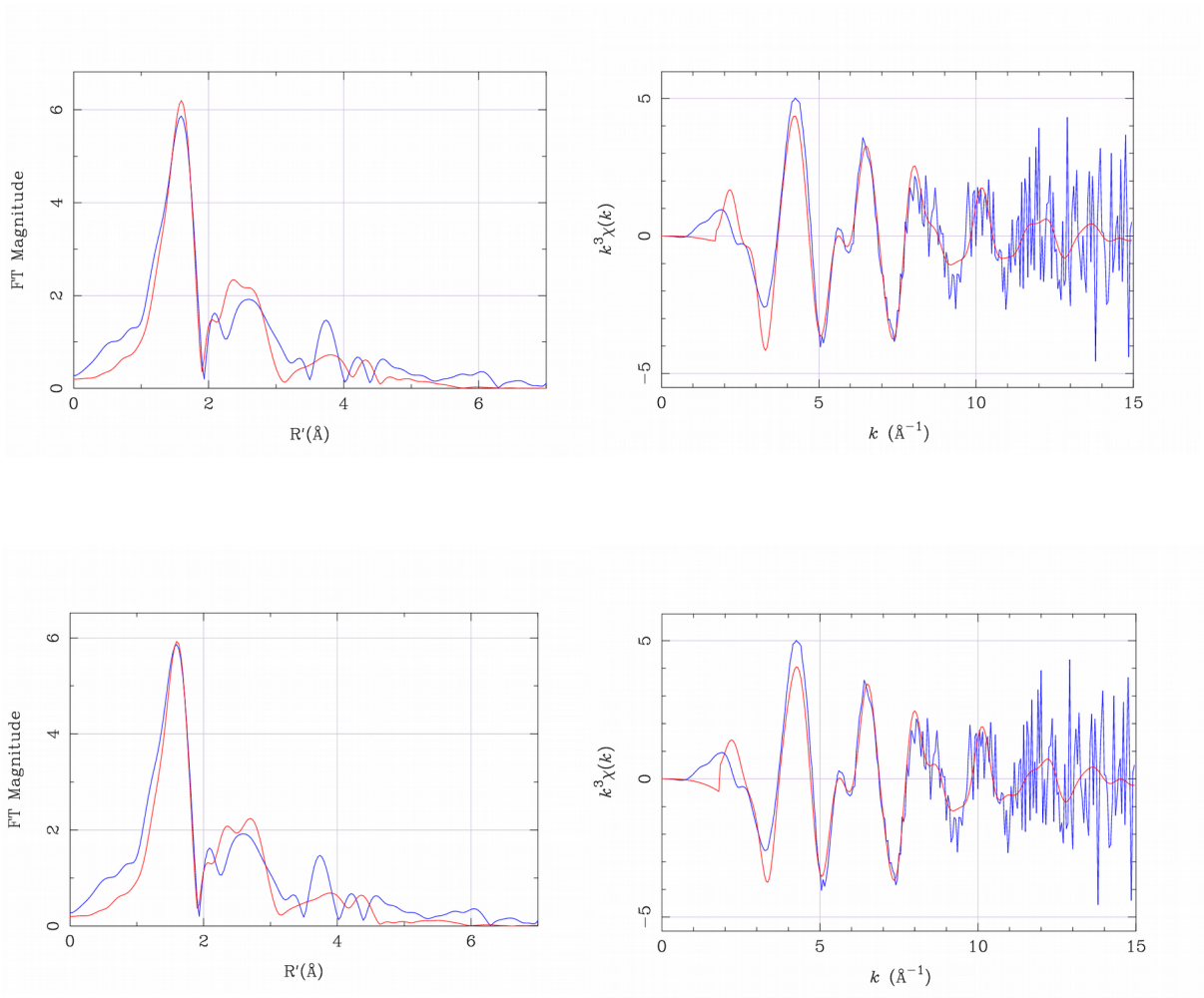

Figure 4. Comparison between the EXAFS raw data (blue) and the fit to the cis-2 complex (a) and the 0.45 $CuAn_4$ + 0.45 $CuPorAn_2$ mixture (b), involving E_0, and Cu–N distances and DWFs of the first-sphere paths (2 in (a) and 3 in (b)), as well as a single DWF for all the other paths (red), displayed as Fourier-transformed magnitude (k^3-weighted, no phase correction) vs. R', and $k^3\chi(k)$ vs. k.